

# Modeling Relative Permeability Effects in Gas-Condensate Reservoirs With a New Trapping Model

G.A. Pope, SPE, W. Wu,\* SPE, G. Narayanaswamy,\*\* SPE, M. Delshad, SPE, M.M. Sharma, SPE, and P. Wang, SPE, The U. of Texas at Austin

## Summary

Many gas-condensate wells show a significant decrease in productivity once the pressure falls below the dew point pressure. A widely accepted cause of this decrease in productivity index is the decrease in the gas relative permeability due to a buildup of condensate in the near wellbore region. Predictions of well inflow performance require accurate models for the gas relative permeability. Since these relative permeabilities depend on fluid composition and pressure as well as on condensate and water saturations, a model is essential for both interpretation of laboratory data and for predictive field simulations as illustrated in this article.

## Introduction

Afidick *et al.*<sup>1</sup> and Barnum *et al.*<sup>2</sup> have reported field data which show that under some conditions a significant loss of well productivity can occur in gas wells due to near wellbore condensate accumulation. As pointed out by Boom *et al.*,<sup>3</sup> even for lean fluids with low condensate dropout, high condensate saturations may build up as many pore volumes of gas pass through the near wellbore region. As the condensate saturation increases, the gas relative permeability decreases and thus the productivity of the well decreases. The gas relative permeability is a function of the interfacial tension (IFT) between the gas and condensate among other variables. For this reason, several laboratory studies<sup>3-14</sup> have been reported on the measurement of relative permeabilities of gas-condensate fluids as a function of interfacial tension. These studies show a significant increase in the relative permeability of the gas as the interfacial tension between the gas and condensate decreases. The relative permeabilities of the gas and condensate have often been modeled directly as an empirical function of the interfacial tension.<sup>15</sup> However, it has been known since at least 1947<sup>16</sup> that the relative permeabilities in general actually depend on the ratio of forces on the trapped phase, which can be expressed as either a capillary number or Bond number. This has been recognized in recent years to be true for gas-condensate relative permeabilities.<sup>8,10</sup> The key to a gas-condensate relative permeability model is the dependence of the critical condensate saturation on the capillary number or its generalization called the trapping number. A simple two-parameter capillary trapping model is presented that shows good agreement with experimental data. This model is a generalization of the approach first presented by Delshad *et al.*<sup>17</sup> We then present a general scheme for computing the gas and condensate relative permeabilities as a function of the trapping number, with only data at low trapping numbers (high IFT) as input, and have found good agreement with the experimental data in the literature. This model, with typical parameters for gas condensates, was used in a compositional simulation study of a single well to better understand the productivity index (PI) behavior of the well and to evaluate the significance of condensate buildup.

## Model Description

The fundamental problem with condensate buildup in the reservoir is that capillary forces can retain the condensate in the pores unless the forces displacing the condensate exceed the capillary forces. To the degree that the pressure forces in the displacing gas phase and the buoyancy force on the condensate exceed the capillary force on the condensate, the condensate saturation will be reduced and the gas relative permeability increased. Brownell and Katz<sup>16</sup> and others recognized early on that the residual oil saturation should be a function of the ratio of viscous to interfacial forces and defined a capillary number to capture this ratio. Since then many variations of the definition have been published,<sup>17-20</sup> with some of the most common ones written in terms of the velocity of the displacing fluid, which can be done by using Darcy's law to replace the pressure gradient with velocity. However, it is the force on the trapped fluid that is most fundamental and so we prefer the following definition:

$$N_{c_l} = \frac{|\vec{k} \cdot \vec{\nabla} \Phi_l|}{\sigma_{ll'}}, \quad (1)$$

where definitions and dimensions of each term are provided in the nomenclature. Although the distinction is not usually made, one should designate the displacing phase  $l'$  and the displaced phase  $l$  in any such definition. In some cases, buoyancy forces can contribute significantly to the total force on the trapped phase. To quantify this effect, the Bond number was introduced and it also takes different forms in the literature.<sup>20</sup> One such definition is as follows:

$$N_{B_l} = \frac{k g (\rho_{l'} - \rho_l)}{\sigma_{ll'}}. \quad (2)$$

For special cases such as vertical flow, the force vectors are collinear and one can just add the scalar values of the viscous and buoyancy forces and correlate the residual oil saturation with this sum, or in some cases one force is negligible compared to the other force and just the capillary number or Bond number can be used by itself. This is the case with most laboratory studies including the recent ones by Boom *et al.*<sup>3,8</sup> and by Henderson *et al.*<sup>10</sup> However, in general the forces on the trapped phase are not collinear in reservoir flow and the vector sum must be used. A generalization of the capillary and Bond numbers was derived by Jin<sup>21</sup> and called the trapping number. The trapping number for phase  $l$  displaced by phase  $l'$  is defined as follows:

$$N_{T_l} = \frac{|\vec{k} \cdot (\vec{\nabla} \Phi_{l'} + g(\rho_{l'} - \rho_l) \vec{\nabla} D)|}{\sigma_{ll'}}. \quad (3)$$

This definition does not explicitly account for the very important effects of spreading and wetting on the trapping of a residual phase. However, it has been shown to correlate very well with the residual saturations of the nonwetting, wetting, and intermediate-wetting phases in a wide variety of rock types.

The residual saturation is modeled based on the trapping number as shown below.

$$S_{lr} = \min \left( S_l, S_{lr}^{\text{high}} + \frac{S_{lr}^{\text{low}} - S_{lr}^{\text{high}}}{1 + T_l(N_{T_l})^{\eta_l}} \right). \quad (4)$$

\*Now with Chinese Petroleum Corp.

\*\*Now with Arco E&P Technology.

Copyright © 2000 Society of Petroleum Engineers

This paper (SPE 62497) was revised for publication from paper SPE 49266, prepared for presentation at the 1998 SPE Annual Technical Conference and Exhibition, New Orleans, 27–30 September. Original manuscript received for review 19 January 1999. Revised manuscript received 5 January 2000. Paper peer approved 20 January 2000.

The trapping parameters  $T_l$  and  $\tau_l$  are obtained by fitting residual saturation data for phase  $l$ .  $S_{lr}^{\text{high}}$  is typically zero and  $\tau_l$  is typically 1.0, however, some of the condensate data from the literature can be fit somewhat better by using  $\tau_l$  as a second fitting parameter. Mass transfer can reduce the value of  $S_l$  to values less than  $S_{lr}$  which is the reason why the minimum is taken in Eq. 4. For example, dry gas flowing by residual condensate at a fixed pressure can strip the lighter components from the condensate and reduce its saturation.

Establishing the correlation of residual saturations with the trapping number (or special cases of it as appropriate) is the first and most fundamental step in correlating relative permeability data as a function of interfacial tension. Although we have always found Eq. 4 to be adequate and convenient for this purpose for a wide variety of data sets including gas condensates, a table could also be used to represent the decrease in residual saturations with increasing trapping number or, for that matter, some other simple function that fits the data. In cases such as gas condensates there are three residual phases (gas, condensate, and water) and this correlation has been found to apply to all three phases.

The next step is to correlate the endpoint relative permeability of each phase, which increases in a very predictable way as the trapping number increases and can be correlated using the following equation:

$$k_{rl}^0 = k_{rl}^0 \text{ low} + \frac{S_{lr}'^{\text{low}} - S_{lr}'^{\text{high}}}{S_{lr}'^{\text{low}} - S_{lr}'^{\text{high}}} (k_{rl}^0 \text{ high} - k_{rl}^0 \text{ low}), \quad (5)$$

where  $S_{lr}'$  is the residual saturation of the conjugate phase, e.g., the condensate is the conjugate phase for gas. This equation has also been found to provide a good correlation of a wide variety of data. All the parameters with the superscript low and high are constants for a specific rock and fluid pairs.

The final step is to calculate the relative permeability of each phase  $l$  as a function of saturation. One approach to this problem is to assume a simple function such as a Corey-type relative permeability function.<sup>17</sup> This then requires correlating the Corey exponent with the trapping number. Eq. 5, written in terms of the exponent rather than the endpoint, can be used for this purpose.<sup>22</sup> However, not all relative permeability data can be fit with a Corey-type model, so we have generalized our approach by using the following equation:

$$\log k_{rl} = \log k_{rl}^0 + \log \bar{S}_l + \frac{\log \left( \frac{k_{rl}}{k_{rl}^0} \right)^{\text{low}} - \log \bar{S}_l}{1 + T_{l'} (N_{T_{l'}})^{\tau_{l'}}}. \quad (6)$$

The normalized saturations ( $\bar{S}_l$ ) in the above equation are defined as

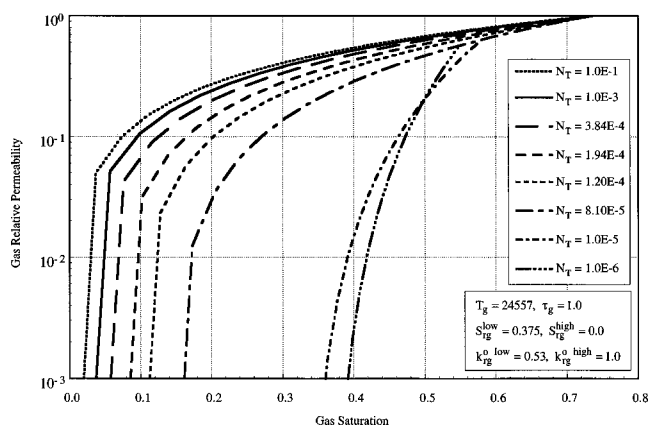


Fig. 1—Gas relative permeabilities calculated from the trapping number model.

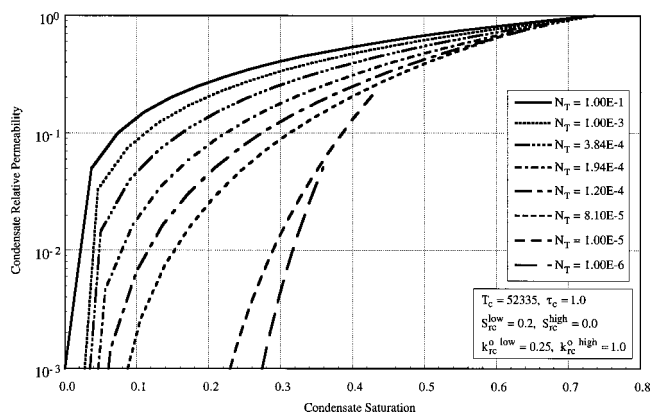


Fig. 2—Condensate relative permeabilities calculated from the trapping number model.

$$\bar{S}_l = \frac{S_l - S_{lr}}{1 - \sum_{l=1}^{n_p} S_{lr}}, \quad (7)$$

where  $n_p$  is the number of phases present,  $S_l$  is the saturation, and  $S_{lr}$  is the residual saturation for phase  $l$ , which are calculated using Eq. 4.

Only the baseline relative permeability curve of each phase at low trapping number corresponding to the usual laboratory measurements and the residual saturations as a function of the trapping number are needed in this approach. Figs. 1 and 2 show the relative permeability of gas and condensate calculated for a wide range of trapping numbers using just two parameters ( $T_{l'}$  and  $\tau_{l'}$ ). The model presented captures the general trends in the data very well and it should be a great improvement over the traditional approach used in compositional reservoir simulators that are used to model gas-condensate reservoirs.

## Comparisons with Experimental Data

As pointed out above, the best starting point for understanding and modeling relative permeability data as a function of interfacial tension is the relationship between the residual saturations and trapping number (or its special cases of capillary number or Bond number when appropriate to the experimental conditions). For this reason, we first show an example of normalized residual saturations vs. trapping number in Fig. 3. The residual saturations were normalized by dividing them by the low trapping number plateau values. As seen from these data, there is a very large difference between the nonwetting and wetting phase data. A much larger trapping number is required to decrease the residual saturation for the wetting phase than for the nonwetting phase. This is typical of all of the data in the literature for all types of

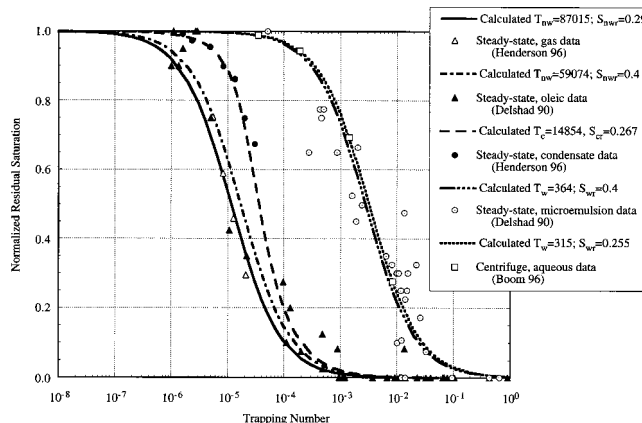


Fig. 3—Effect of wettability on the desaturation curves for Berea sandstone.

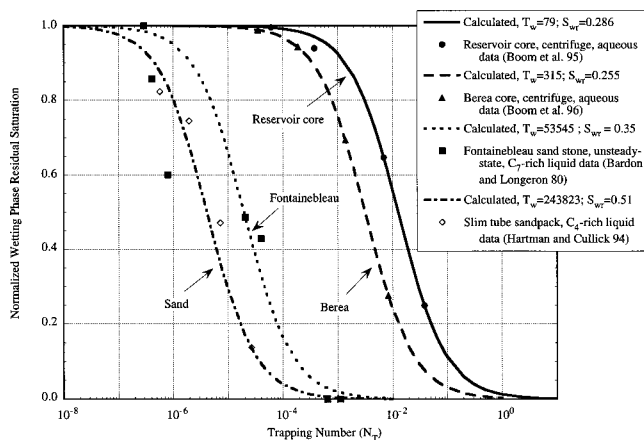


Fig. 4—Comparison of model with experimental wetting phase residual saturation data for various porous media.

phases and rocks (e.g., see the review in Ref. 22). We selected these data from the many examples in the literature to make the point that even widely different phases have similar behavior in a given rock if their wettability is the same. The nonwetting phases in Fig. 3 are the gas and oil. The gas data of Henderson *et al.*<sup>10</sup> are for the equilibrium gas in a binary mixture of methane and *n*-butane intended to represent a gas-condensate fluid. The oil data of Delshad<sup>22</sup> are for the equilibrium oil for a mixture of decane, brine, isobutanol, and sodium sulfonate under three-phase conditions. The wetting phases in Fig. 3 are the aqueous and microemulsion phases. The aqueous data of Boom *et al.*<sup>3,8</sup> are for the equilibrium aqueous phase in a ternary mixture of water, *n*-heptane, and isopropyl alcohol. The microemulsion data of Delshad<sup>22</sup> are for the equilibrium microemulsion. The condensate data of Henderson *et al.*<sup>10</sup> appear to be of intermediate wettability (between the gas and water), which emphasizes the importance of including all three phases in the experiments.

More examples of wetting phase data for several different porous media are shown in Fig. 4. The corresponding data for the nonwetting phase are shown in Fig. 5. These data emphasize the strong dependence on the rock as well as on the wettability of the phases. The overwhelming conclusion is that one must measure the residual saturations for the wetting state and rock of interest to get useful results that can be accurately applied to a particular reservoir state. In particular, if there are three phases in the reservoir such as there are with gas condensates then, to ensure the correct wetting and spreading state in the rock, three phases need to be in the laboratory core even if one of the phases such as the brine is always at residual saturation. There are too many other similar examples in the literature to review here, but many other

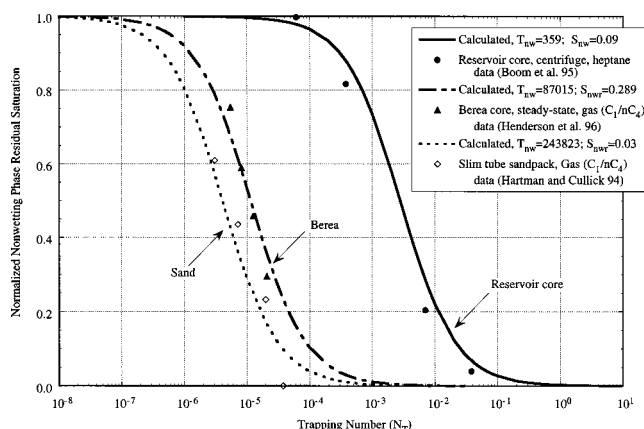


Fig. 5—Comparison of model with experimental nonwetting phase residual saturation data for various porous media.

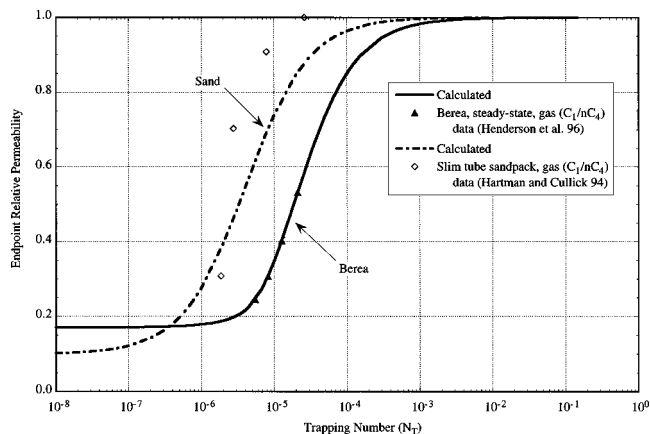


Fig. 6—Comparison of model with experimental nonwetting phase endpoint relative permeability data for various porous media.

data sets can be found in the work of Stegemeier,<sup>23</sup> Chatzis and Morrow,<sup>24</sup> Delshad,<sup>22</sup> and Filco and Sharma<sup>25</sup> among others. Stegemeier<sup>23</sup> provides an excellent theoretical treatment as well.

All of the data shown in Figs. 3 through 5 were fit using just one parameter,  $T_l$ , for each phase,  $l$ , and the value of this parameter is shown in each figure. Next we show the comparisons with endpoint relative permeabilities using these same values of  $T_l$ . Fig. 6 shows the endpoint relative permeability of the gas phase as a function of trapping number for the methane/*n*-butane binary mixture reported by both Hartman and Cullick<sup>7</sup> and Henderson *et al.*<sup>10</sup> Fig. 7 shows the endpoint relative permeability for various liquid phases and porous media as a function of the trapping number. The values vary significantly due to the differing rocks and for the same rock such as Berea sandstone due to the differing wettability. However, the general trend of increasing endpoint relative permeability with increasing trapping number is consistent and clear and agrees with that previously reported by Delshad *et al.*<sup>17</sup> for widely different fluids.

The curve calculated from Eq. 5 of the model is shown for comparison with these data. In all of these cases, the endpoint relative permeability appears to approach 1.0 at a sufficiently high trapping number. This high trapping number value is sometimes referred to as the miscible value, but, strictly speaking, it is still an immiscible value even if the interfacial tension is ultralow. As shown by Delshad,<sup>22</sup> the interfacial tension can be high and the trapping number still made high enough in the laboratory by increasing the pressure gradient to make the endpoint approach one, so it is not the interfacial tension that matters per se, but rather the trapping number. The endpoint relative permeability was not al-

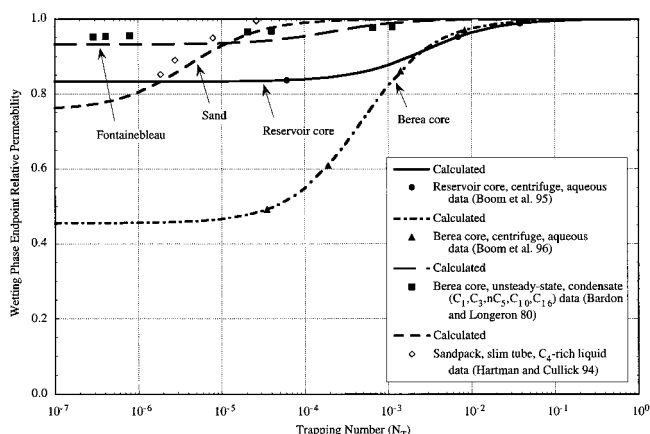


Fig. 7—Comparison of model with experimental wetting phase endpoint relative permeability data for various porous media.

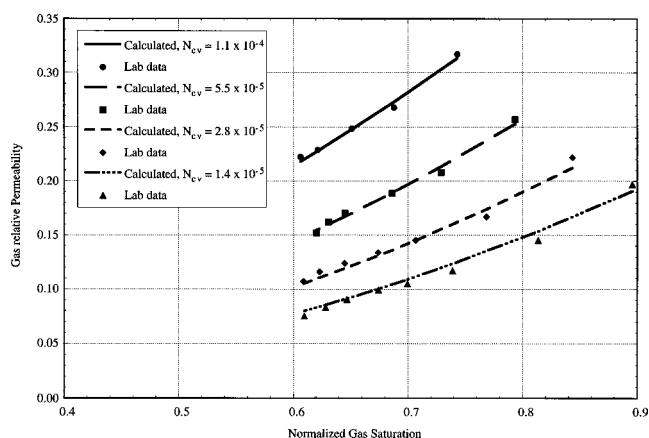


Fig. 8—Comparison of calculated and experimental gas relative permeability data (Ref. 10).

ways measured by these investigators at a sufficiently low value of trapping number to determine its value directly, so its value had to be estimated by fitting the available data at intermediate trapping numbers. This value is often referred to as the immiscible value of the endpoint, but clearly this is not a useful designation. Its value depends on the value of the trapping number. In some cases, a plateau value of the endpoint at some sufficiently low trapping number is observed, but this is not always the case, especially for heterogeneous rocks and any phase that is wetting or even mixed wet. For these and other fundamental reasons, the designations of miscible and immiscible are not correct or useful, nor is it meaningful to describe these data in terms of high and low interfacial tension, but rather only in terms of high or low trapping number.

Figs. 8 through 11 show comparisons between the model curves and several sets of relative permeability data for gas and condensate fluids. No new parameters were introduced and yet all of the trends in the data are captured reasonably well. The capillary numbers shown in Figs. 8 and 9 correspond to the definition used by Henderson *et al.*,<sup>10</sup> which is based upon velocity rather than the potential gradient. Since their experiments were done with their capillary number held constant, it made more sense to plot these relative permeability data using their definition. Under their experimental conditions, buoyancy was negligible, so our model could be used with either definition of capillary number. In general, however, the trapping number should be used.

It is important to note that very few parameters are needed in this model and that it goes to all of the correct limits observed not just for these data but for other literature data for various cores, fluids, and conditions. Our modeling efforts show that for reason-

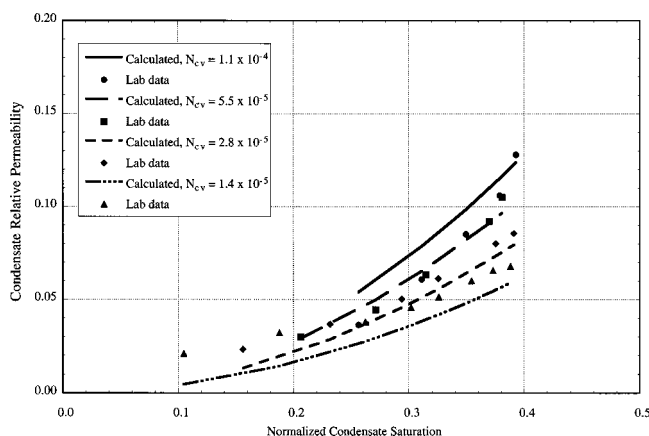


Fig. 9—Comparison of calculated and experimental condensate relative permeability data (Ref. 10).

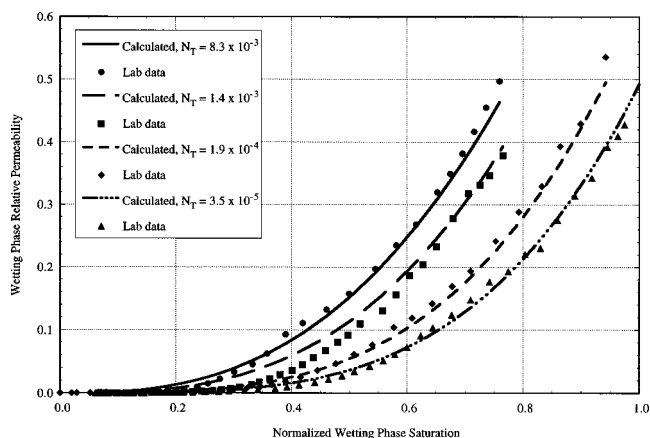


Fig. 10—Comparison of calculated and experimental wetting phase relative permeability data (Ref. 3).

able prediction of relative permeability at various trapping numbers, the measurement of endpoint relative permeabilities at different trapping numbers is more important than the measurement of relative permeabilities at various saturations at different trapping numbers.

### Numerical Simulations

We used the relative permeability curves of Figs. 1 and 2 to investigate the effect of trapping number on the productivity of a single well in a gas-condensate reservoir. The equation-of-state (EOS) compositional reservoir simulator UTCOMP was used in this study.<sup>26</sup> The fluid description and phase behavior are the same as those given by Wu *et al.*<sup>27</sup> For simplicity, a layered-permeability description was used for this initial simulation study. Both the reservoir description and phase behavior are similar to those of the Arun field studied by Afidick *et al.*<sup>1</sup> However, these simulations are not meant to apply to the Arun field, but rather were done simply to illustrate the trends in the PI with trapping number. A systematic simulation study of the Arun field including a history match of the PI can be found in Refs. 28 and 29.

### Description of the Simulation Data

The simulation domain used was a two-dimensional radial cross section ( $x$ - $z$ ) with a fan shape at an angle of  $36^\circ$  (Fig. 12). The simulation grid has eight layers (Table 1) with the highest permeability layer at the top (90 md) and the lowest permeability layer at the bottom (1.5 md). The vertical permeability was one tenth that in the horizontal direction. Nineteen gridblocks were used in the  $x$  direction with a variable gridblock size of 1 to 500 ft and with the smaller gridblocks located near the wellbore. The well is

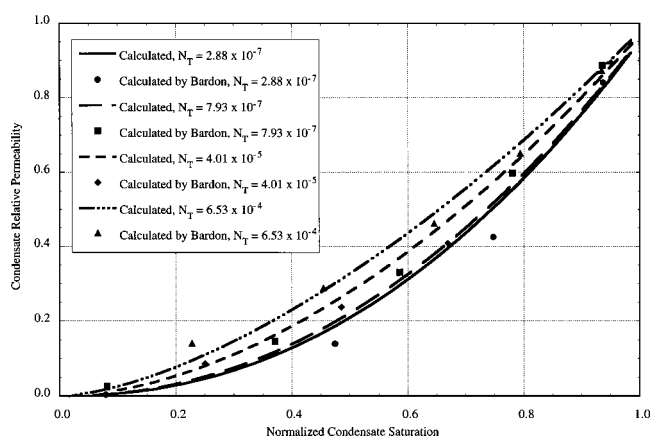


Fig. 11—Comparison of calculated and experimental condensate relative permeability data (Ref. 6).



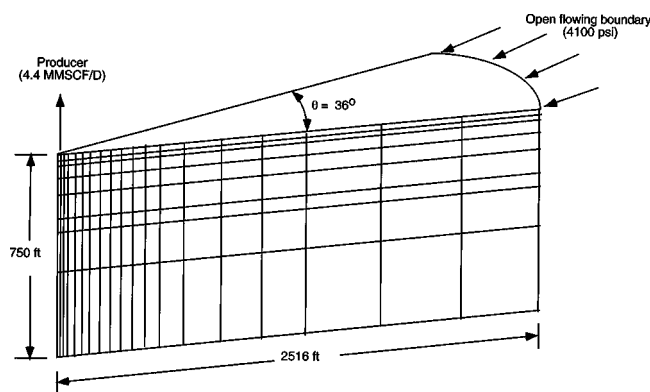


Fig. 12—Schematic of the gridding scheme used in the simulation study.

producing at a constant rate of  $4.4 \times 10^6$  scf/D (which corresponds to one tenth of the full well rate) and it penetrates all eight layers. A constant pressure (4,100 psia) boundary condition was applied to the outer boundary of the fan-shaped reservoir, and this allows fluid with the initial composition to flow into the simulation domain. The reservoir temperature and pressure are 335°F and 4,100 psia, so the initial fluid composition is in the two-phase region since the dew point pressure is about 4,408 psi.

### Discussion of Results

We performed simulations with and without the effects of trapping number on the relative permeability to demonstrate its significance on condensate saturation and PI. Figs. 13 and 14 illustrate the distribution of condensate with and without the effect of trapping number. Fig. 13 shows that the condensate saturation goes through a maximum with distance from the well in the high permeability layers. This is because the trapping number results in low values of condensate saturation very close to the well in the high permeability layers; then the condensate saturation increases as the trapping number decreases with increasing distance from the well, and it finally decreases again due to the increase in the pressure. The maximum condensate saturation occurs farther from wellbore in the top (high permeability) layers. Fig. 14 shows the condensate saturation in the near wellbore region for the case without the trapping number modeled is high near the well and then decreases away from the well in all layers.

Fig. 15 illustrates the range of trapping numbers encountered in both the top and bottom layers for the simulation as a function of distance from the wellbore. In the top layer, trapping numbers are above the critical trapping number (about  $10^{-6}$  in Fig. 3) for up to the 100 ft from the wellbore. In the bottom layer that has the lowest permeability, no increase in relative permeability due to trapping number effects will be seen because the trapping number is less than the critical trapping number.

Fig. 16 shows the condensate saturation in layer 1 as a function of distance from the well with and without the trapping number modeled and for two values of endpoint gas relative permeability.

TABLE 1—RESERVOIR DESCRIPTION			
Layer	Thickness (ft)	Porosity (fraction)	Permeability (md)
1	10	0.300	90
2	10	0.250	75
3	30	0.214	50
4	50	0.220	28
5	100	0.209	12
6	50	0.219	17
7	150	0.127	2.6
8	370	0.120	1.5

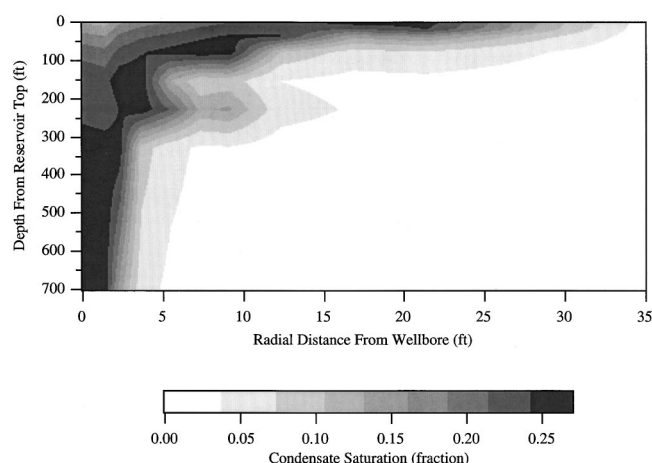


Fig. 13—Condensate saturation map at 60 days (including trapping number effects).

The variations in condensate saturation are more significant in the lower endpoint gas relative permeability. The use of 0.2 as the endpoint gas relative permeability enlarges the range of relative permeabilities and hence more significant effects of the trapping number are observed.

The normalized well productivity index, with and without trapping number and for two different gas endpoints, is shown in Fig. 17 as a function of the average reservoir pressure. The PI in this study was computed using the following equation:

$$PI = \frac{Q}{P_{ave} - P_{wf}}, \quad (8)$$

where  $Q$  is in millions of scf/D and  $P_{ave}$  and  $P_{wf}$  are in psia. The ratio of the PI to the initial PI gives the normalized PI. The initial productivity index was taken at 0.01 days for each case.

Fig. 17 shows that the PI decreases rapidly as condensate builds up in the reservoir, but that the effect is somewhat attenuated when the reduction in condensate saturation at high values of trapping number is modeled. The trapping number effect is more significant for the case of low endpoint gas relative permeability than for the higher value. After a certain period of production, the difference in the productivity between these two runs is almost unchanged: the well productivity in the run with trapping number effects remains about 35% higher for the case with an endpoint of 0.53. The productivity modeled with the trapping number is approximately twice that without trapping number when using the low endpoint gas curve (0.2). Table 2 lists the productivity index for the partial well in each layer with and without trapping num-

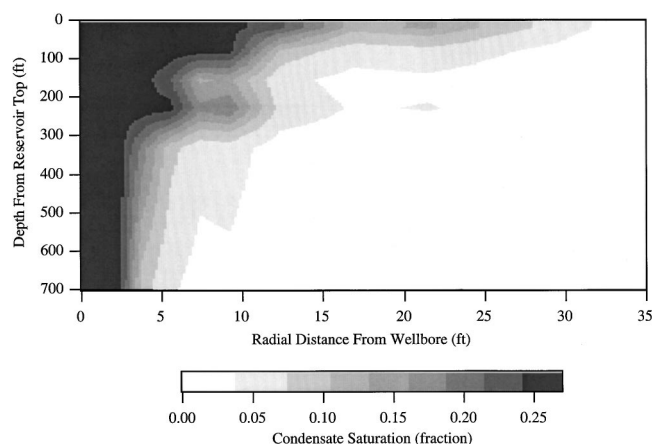


Fig. 14—Condensate saturation map at 60 days (without trapping number effects).

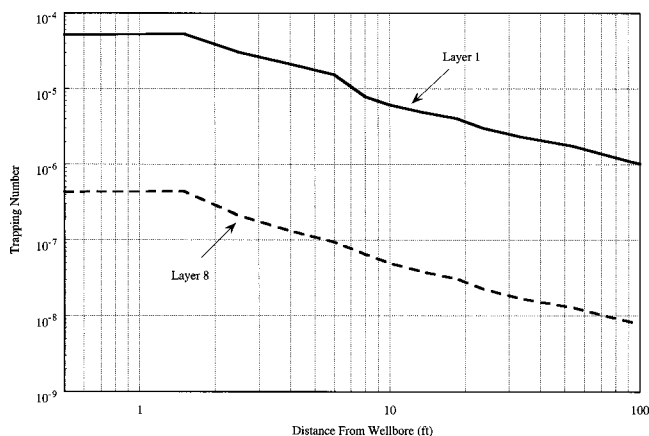


Fig. 15—Trapping number as a function of distance from the wellbore for the highest and lowest permeability layers.

ber effects after 10 days of production. The layer-averaged pressure and bottomhole pressure at each layer were used for the  $P_{ave}$  and  $P_{wf}$  in Eq. 8. It can be seen from Table 2 that the productivity index is more than two times greater in the top two layers when trapping number effects are modeled. The productivity index decreases as the formation permeability decreases. In the bottom two layers, no significant effects of the trapping number on the productivity index were observed.

This simulation study shows why relative permeability should not be modeled based on IFT only. The fundamental nature of changes in relative permeability was shown using the trapping number concept. The basic equations clearly indicate that IFT is not the only factor affecting residual saturations and the critical condensate saturation in particular. Hence, the crucial rate effects that contribute significantly in the near wellbore region will not be accounted for by an IFT model. The reduction in condensate saturation in high permeability layers near the wellbore will not be shown by such a model. Conditions in the near wellbore region for high permeability layers are the most important factors affecting the PI. Hence, relative permeability models based on IFT only have a very poor chance of making accurate predictions of the PI. Furthermore, it would be very difficult to model all of these interacting effects analytically since heterogeneity, pressure, phase behavior, interfacial tension, trapping number, and relative permeability are all coupled in a complex and nonlinear way. The coupling with heterogeneity is strong even when the reservoir description is very simple as in this example. Simulations have been conducted using stochastically generated permeability fields to further elucidate this coupling for more realistic reservoir descriptions.<sup>28</sup> Assuming a uniform condensate buildup close to

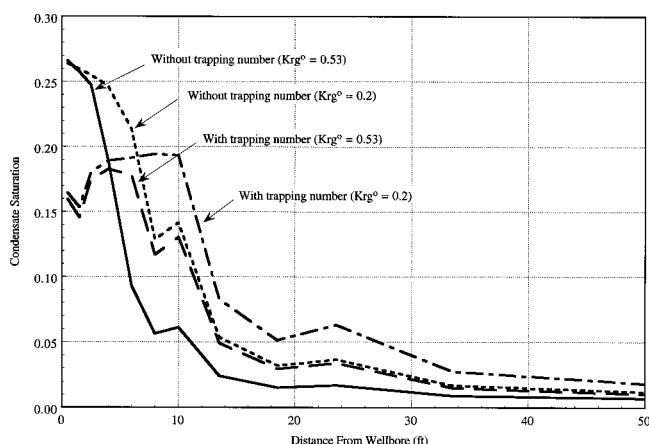


Fig. 16—Condensate saturation for layer 1.

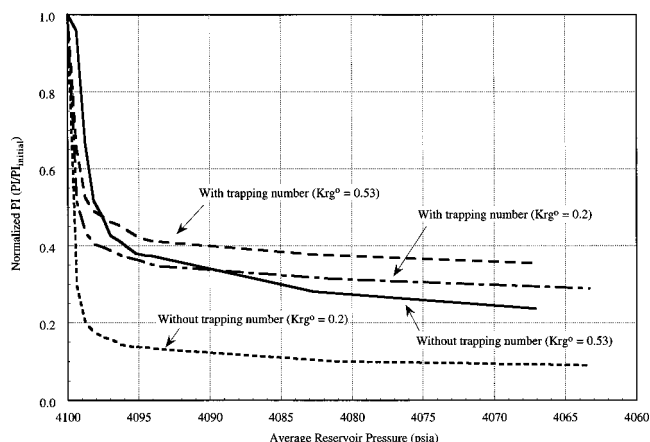


Fig. 17—Normalized productivity index.

the wellbore is not correct and does not lead to accurate predictions, nor is it reasonable to assume there is a donut-shaped condensate bank near the wellbore.

In addition, for simplicity and clarity, we did not include non-Darcy effects in this illustrative simulation, but for very high rate gas wells, non-Darcy flow can be significant and is also coupled with all of the above variables and should be taken into account.<sup>28,30,31</sup>

## Summary and Conclusions

The buildup of condensate close to gas-condensate wells can significantly reduce the gas relative permeability and thus the PI of the well and must be accounted for with an accurate relative permeability model. Although interfacial tension can be low and variable and does affect the gas and condensate relative permeabilities, it is not correct or accurate to model the relative permeabilities directly as a function of interfacial tension, but rather they should be modeled as a function of the combined effects of pressure gradient, buoyancy, and capillary forces. This requires generalization of the classical capillary number and Bond number into a trapping number. As was shown in this article, the trapping number can be used in a generalized relative permeability model to correlate gas-condensate data and then used in a simulator to predict changes in the PI due to changes in condensate saturation.

## Nomenclature

- $D$  = depth, L
- $g$  = gravitational constant,  $Lt^{-2}$
- $\vec{k}$  = permeability tensor,  $L^2$
- $k_{rl}$  = relative permeability of phase  $l$
- $k_{rl}^0$  = endpoint relative permeability of phase  $l$
- $k_{rl}^{0 \text{ high}}, k_{rl}^{0 \text{ low}}$  = phase  $l$  endpoint relative permeability at high and low trapping numbers

TABLE 2—PRODUCTIVITY INDEX (MILLIONS OF scf/D/psi)

Layer	$K_{rg}^0 = 0.53$		$K_{rg}^0 = 0.2$	
	With $N_T$	Without $N_T$	With $N_T$	Without $N_T$
1	16.486	8.244	9.541	2.825
2	13.120	6.868	7.474	2.353
3	23.739	13.732	12.983	4.779
4	20.008	12.801	10.116	4.895
5	16.300	13.120	7.050	4.358
6	12.931	8.482	6.446	3.095
7	4.839	5.705	1.856	1.687
8	7.433	7.933	3.346	2.780

$N_{B_l}$  = bond number of phase  $l$   
 $N_{c_l}$  = capillary number of phase  $l$   
 $N_{T_l}$  = trapping number of phase  $l$   
 $n_p$  = number of phases  
 $P_{ave}$  = average reservoir pressure,  $\text{mL}^{-1} \text{t}^{-2}$   
 $P_{wf}$  = bottomhole flowing pressure,  $\text{mL}^{-1} \text{t}^{-2}$   
 $P_l$  = pressure of phase  $l$ ,  $\text{mL}^{-1} \text{t}^{-2}$   
 $PI$  = productivity index,  $\text{L}^3 \text{t}^{-1} / \text{mL}^{-1} \text{t}^{-2}$   
 $Q$  = total production rate,  $\text{L}^3 \text{t}^{-1}$   
 $S_l$  = saturation of phase  $l$ ,  $\text{L}^3 / \text{L}^3$  PV  
 $S_{lr}$  = residual saturation of phase  $l$ ,  $\text{L}^3 / \text{L}^3$  PV  
 $S_{lr}^{0 \text{ high}}, S_{lr}^{0 \text{ low}}$  = residual saturation of phase  $l$  at high and low  $N_T$ ,  $\text{L}^3 / \text{L}^3$  PV  
 $T_l$  = trapping parameter for phase  $l$

## Greek Symbols

$\vec{\nabla} \Phi_{l'}$  = flow potential gradient given by  
 $\vec{\nabla} P_{l'} - g \rho_{l'} \vec{\nabla} D$   
 $\rho_l$  = density of phase  $l$ ,  $\text{mL}^{-3}$   
 $\sigma_{ll'}$  = interfacial tension between phases  $l$  and  $l'$ ,  $\text{m}^2$   
 $\Phi_l$  = potential of phase  $l$ ,  $\text{mL}^{-1} \text{t}^{-2}$   
 $\tau_l$  = trapping model parameter

## Subscripts

$l$  = displaced phase  
 $l'$  = displacing phase  
 $r$  = residual

## Superscripts

high = high trapping number  
 low = low trapping number  
 0 = end point

## Acknowledgments

We thank Mobil for funding this research project and specifically thank the members of the gas-condensate team at Mobil Exploration and Production Technical Center (MEPTC): Kathy Hartman, Myung Hwang, Ravi Vaidya, Jim Dixon, Steve Weber, and Mary Coles for useful discussions and suggestions during the course of this research. We also wish to thank Rene Frederiksen for his help with some of the model calculations.

## References

- Afidick, D., Kaczorowski, N.J., and Bette, S.: "Production Performance of a Retrograde Gas: A Case Study of the Arun Field," paper SPE 28749 presented at the 1994 Asia Pacific Oil and Gas Conference, Melbourne, Australia, 7–10 November.
- Barnum, R.S. *et al.*: "Gas Condensate Reservoir Behavior: Productivity and Recovery Reduction Due to Condensation," paper SPE 30767 presented at the 1995 SPE Annual Technical Conference and Exhibition, Dallas, 22–25 October.
- Boom, W. *et al.*: "On the Use of Model Experiments for Assessing Improved Gas-Condensate Mobility Under Near-Wellbore Flow Conditions," paper SPE 36714 presented at the 1996 SPE Annual Technical Conference and Exhibition, Denver, Colorado, 6–9, October.
- Asar, H. and Handy, L.L.: "Influence of Interfacial Tension on Gas/Oil Relative Permeability in a Gas-Condensate System," *SPE* (February 1988) 257.
- Hanif, M.S. and Ali, J.K.: "Relative Permeability and Low Tension Fluid Flow in Gas Condensate Systems," paper SPE 20917 presented at the 1990 European Petroleum Conference, The Hague, The Netherlands, 22–24 October.
- Bardon, C. and Longeron, D.G.: "Influence of Very Low Interfacial Tensions on Relative Permeability," *SPEJ* (October 1980) 391.
- Hartman, K.J. and Cullick, A.S.: "Oil Recovery by Gas Displacement at Low Interfacial Tension," *J. Pet. Sci. Eng.* (1994) 10, 197.
- Boom, W. *et al.*: "Experimental Evidence for Improved Condensate Mobility at Near-Wellbore Flow Conditions," paper SPE 30766 presented at the 1995 SPE Annual Technical Conference and Exhibition, Dallas, 22–25 October.
- Chen, H.L., Monger-McClure, T.G., and Wilson, S.D.: "Determination of Relative Permeability and Recovery for North Sea Gas Condensate Reservoirs," paper SPE 30769 presented at the 1995 SPE Annual Technical Conference and Exhibition, Dallas, 22–25 October.
- Henderson, G.D. *et al.*: "Measurement and Correlation of Gas Condensate Relative Permeability by the Steady-State Method," *SPE* (April 1998) 134.
- Kalaydjian, F.J.M., Bourbiaux, B.J., and Lombard, J.M.: "Predicting Gas-Condensate Reservoir Performance: How Flow Parameters Are Altered When Approaching Production Wells," paper SPE 36715 presented at the 1996 SPE Annual Technical Conference, Denver, Colorado, 6–9 October.
- Ali, J.K., McGauley, P.J., and Wilson, C.J.: "The Effects of High-Velocity Flow and PVT Changes Near the Wellbore on Condensate Well Performance," paper SPE 38923 presented at the 1997 SPE Annual Technical Conference and Exhibition, San Antonio, Texas, 5–8 October.
- Morel, D.C., Nectoux, A., and Danquigny, J.: "Experimental Determination of the Mobility of Hydrocarbon Liquids During Gas Condensate Reservoir Depletion: Three Actual Cases," paper SPE 38922 presented at the 1997 SPE Annual Technical Conference and Exhibition, San Antonio, Texas, 5–8 October.
- McDougall, S.R., Salino, P.A., and Sorbie, K.S.: "The Effect of Interfacial Tension Upon Gas-Oil Relative Permeability Measurements: Interpretation Using Pore-Scale Models," paper SPE 38920 presented at the 1997 SPE Annual Technical Conference and Exhibition, San Antonio, Texas, 5–8 October.
- Coats, K.H.: "An Equation of State Compositional Model," *SPEJ* (1980) 20, 363.
- Brownell, L.E. and Katz, D.L.: "Flow of Fluids Through Porous Media—Part II," *Chem. Eng. Prog.* (1947) 43, No. 11, 601.
- Delshad, M. *et al.*: "Effects of Capillary Number on the Residual Saturation of Three Phase Micellar Solution," paper SPE 14911 presented at the 1986 SPE/DOE Symposium on Enhanced Oil Recovery, Tulsa, Oklahoma, 20–23 April.
- Lake, L.W.: *Enhanced Oil Recovery*, Prentice-Hall, Englewood Cliffs, New Jersey (1989).
- Jerauld, G.R.: "General Three-Phase Relative Permeability Model for Prudhoe Bay," *SPE* (November 1997) 255.
- Morrow, N.R. and Songkran, B.: *Surface Phenomena in Enhanced Oil Recovery*, D.O. Shah (ed.), Plenum Press, New York City (1982) 387–411.
- Jin, M.: "A Study of Non-Aqueous Phase Liquid Characterization and Surfactant Remediation," PhD dissertation, The U. of Texas, Austin, Texas (1995).
- Delshad, M.: "Trapping of Micellar Fluids in Berea Sandstone," PhD dissertation, The U. of Texas, Austin, Texas (1990).
- Stegemeier, G.L.: "Mechanisms of Entrapment and Mobilization of Oil in Porous Media," *Improved Oil Recovery by Surfactant and Polymer Flooding*, D.O. Shah and R.S. Schechter (eds.), Academic Press, New York City (1977) 55–91.
- Chatzis, I. and Morrow, N.R.: "Correlation of Capillary Number Relationships for Sandstones," paper SPE 10114 presented at the 1981 Annual SPE Conference, San Antonio, Texas, 5–7 October.
- Filco, P. and Sharma, M.M.: "Effect of Brine Salinity and Crude Oil Properties on Relative Permeabilities and Residual Saturations," paper SPE 49320 presented at the 1998 SPE Annual Technical Conference and Exhibition, New Orleans, 27–30 September.
- Chang, Y.-B., Pope, G.A., and Sepehrnoori, K.: "A Higher-Order Finite-Difference Compositional Simulator," *J. Pet. Sci. Eng.* (1990) 5, 35.
- Wu, W.-J. *et al.*: "Modeling Non-Equilibrium Mass Transfer Effects for a Gas-Condensate Field," paper SPE 39746 presented at the 1998 Asia Pacific Conference, Kuala Lumpur, 23–24, March.
- Narayanaswamy, G.: "Well Deliverability of Gas Condensate Reservoirs," MS thesis, The U. of Texas, Austin, Texas (1998).
- Narayanaswamy, G., Pope, G.A., and Sharma, M.M.: "Predicting Gas-Condensate Well Productivity Using Capillary Number and Non-Darcy Effects," paper SPE 51910 presented at the 1999 SPE Reservoir Simulation Symposium, Houston, 14–17 February.
- Blom, S.M.P. and Hagoort, J.: "The Combined Effect of Near-Critical Relative Permeability and Non-Darcy Flow on Well Impairment by Condensate Drop-Out," paper SPE 39976 presented at the 1998 SPE Gas Technology Symposium, Calgary, 15–18 March.
- Narayanaswamy, G., Sharma, M.M., and Pope, G.A.: "Effect of Heterogeneity on the Non-Darcy Flow Coefficient," *SPE* (June 1999) 296.

---

**SI Metric Conversion Factors**

bbl × 1.589 873	E-01 = m <sup>3</sup>
°F (°F-32)/1.8	= °C
ft × 3.048	E-01 = m
ft <sup>3</sup> /d × 2.831 685	E-03 = m <sup>3</sup> /d
md × 3.008 142	E-04 = μm <sup>2</sup>
psi × 6.894 757	E+00 = kPa

---

**SPEREE**

---

**Gary A. Pope** is Director of the Center for Petroleum and Geosystems Engineering at the U. of Texas at Austin, where he has taught since 1977. e-mail: gary\_pope@pe.utexas.edu. Previously, he worked in Production Research at Shell Development Co. His teaching and research interests include groundwater modeling and remediation, enhanced oil recovery, chemical thermodynamics and phase behavior, and the use of tracers for reservoir characterization. Pope holds a BS degree from Oklahoma State U. and a PhD degree from Rice U., both in chemical engineering. He is a member of the SPE Editorial Review Committee and has served on technical and programming committees. **Wei-Jr Wu** is a petroleum engineer with Chinese Petroleum Corp. Exploration and Development Research Inst. in Taipei, Taiwan. e-mail: wwu@cpcedri.com.tw. Previously, he was a research associate at the Center for Petroleum and Geosystems Engineering at the U. of Texas at Austin. His research interests include chemical flooding, reservoir simulation, and contaminant re-

mediation design and simulation. Wu holds a PhD degree in petroleum and geosystems engineering from the U. of Texas at Austin. **Ganesh Narayanaswamy** is a research engineer in the Reservoir Engineering Analysis Div. at Arco E&P Technology in Plano, Texas. He holds a BS degree in petroleum engineering for the Indian Inst. of Technology, Madras, India, and an MS degree in Petroleum and geosystems engineering from the U. of Texas at Austin. **Mojdeh Delshad** is a research engineer for the Center for Petroleum and Geosystems Engineering at the U. of Texas at Austin. e-mail: mojdeh\_delshad@pe.utexas.edu. She has worked on experimental, modeling, and simulations of improved oil recovery processes in petroleum reservoirs. Delshad holds a PhD degree in petroleum engineering from the U. of Texas at Austin. **Mukul M. Sharma** is Professor of Petroleum, Geosystems, and Chemical Engineering at the U. of Texas at Austin. e-mail: mukul\_sharma@pe.utexas.edu. He has authored more than 140 publications and 4 patents. He holds a BS degree in chemical engineering from IIT Kanpur and MS and PhD degrees in chemical and petroleum engineering from the U. of Southern California. Sharma received the 1998 SPE Formation Evaluation Award; he has served as a Review Chairman for *SPE Formation Evaluation* and as a member of the Editorial Board for *SPE Journal*. **Peng Wang** is a research scientist with the Center for Petroleum and Geosystems Engineering at the U. of Texas at Austin. e-mail: peng\_wang@pe.utexas.edu. Previously, he was a research engineer with Elf Geoscience Research Center in London. His research interests include reservoir simulation and phase behavior of reservoir fluids. Wang holds BS, MS, and PhD degrees in chemical engineering.